DALTON
FULL PAPER

Insertion and cleavage reactions of [*closo*-3,1,2-Ta(NMe_2)$_3$-($C_2B_9H_{11}$)] with nitriles, phenols and thiols; structural characterisation of *N*,*N*-dimethylamidinate ligands †

Charlotte K. Broder, Andrés E. Goeta, Judith A. K. Howard, Andrew K. Hughes,* Andrew L. Johnson, John M. Malget and Ken Wade

Department of Chemistry, University Science Laboratories, South Road, Durham, UK DH1 3LE

Received 19th June 2000, Accepted 25th August 2000
First published as an Advance Article on the web 22nd September 2000

The tantalum complex [*closo*-3,1,2-Ta(NMe_2)$_3$($C_2B_9H_{11}$)] underwent insertion into the NC bond of acetonitrile and *p*-fluorobenzonitrile to give the *N*,*N*-dimethylacetamidinate complex [*closo*-3,1,2-Ta{N=C(Me)NMe_2}$_3$($C_2B_9H_{11}$)], and *p*-fluoro-*N*,*N*-dimethylbenzamidinate, [*closo*-3,1,2-Ta{N=C(C_6H_4F)NMe_2}$_3$($C_2B_9H_{11}$)], respectively. Attempted re-crystallisation of the latter from chlorinated solvents led to [*closo*-3,1,2-Ta{N=C(C_6H_4F)NMe_2}$_2$Cl($C_2B_9H_{11}$)], in which one amidinate ligand has been replaced by a chloride. [*closo*-3,1,2-Ta(NMe_2)$_3$($C_2B_9H_{11}$)] reacts with cyclohexylisocyanide to give [Ta(NMe_2)$_2${η^2-N(Cy)CNMe_2}($C_2B_9H_{11}$)]. The structures of the novel *N*,*N*-dialkylamidinate complexes have been determined by single crystal X-ray diffraction, and reveal the extensive delocalisation and strong π-donor character of the amidinate ligands. The M–N bonds of [*closo*-3,1,2-Ta(NMe_2)$_3$($C_2B_9H_{11}$)] are cleaved by protic reagents, and it reacts with 2,6-dimethylphenol to give [*closo*-3,1,2-Ta($OC_6H_3Me_2$-2,6)$_3$($C_2B_9H_{11}$)] and with benzenethiol to give the charge-compensated complex [*closo*-3-Ta(SC_6H_5)$_4$(9-$NHMe_2$-1,2-$C_2B_9H_{10}$)] where the β-boron of the C_2B_3 face bears a $NHMe_2^+$ substituent. The structures of the last two compounds have also been determined.

Introduction

We recently reported the synthesis and characterisation of the dicarbollide tris(dimethylamide) [*closo*-3,1,2-M(NMe_2)$_3$-($C_2B_9H_{11}$)] (M = Nb, **1** or Ta **2**), together with the insertion of CO_2 and CS_2 into the M–NMe_2 bonds of **1** and **2** to give tris(carbamate) and tris(dithiocarbamate) complexes.[1] These are rare examples of dicarbollide complexes with Group 5 metals,[2,3] and of complexes containing both dicarbollide and amide ligands.[4]

The amminolysis reaction of metal amides with acids is well known,[5] and in recent years has found use as a novel method for ligand co-ordination,[6,7] occasionally providing routes to otherwise inaccessible compounds[8] or thermodynamic product ratios.[9] Thermodynamically, a reaction between a metal amide complex and a Brønsted acid will occur if the acid is more acidic than the eliminated HNR_2, pK_a 35–40. Given that reactions of M–NR_2 bonds with acids are likely to proceed *via* a σ-bond metathesis, involving some prior co-ordination, those of co-ordinating acids such as amines, alcohols and thiols are kinetically more favourable than with carbon acids, such as C_5H_6 or PhCCH.[10]

The other typical reactions of metal amides are insertion into polar multiple bonds. Acetonitrile acts as a Brønsted acid with amides of tin and lead,[11] but inserts into the metal–nitrogen bond of early transition metal amides, M–NR_2, to form *N*,*N*-dialkylamidinate ligands, M–NC(Me)NR_2,[12] occasionally accompanied by the formation of poly(acetonitrile). Although there have been many studies of the isomeric *N*,*N*′-dialkylamidinates,[13] to the best of our knowledge there are no structurally characterised examples of the less numerous *N*,*N*-dialkylamidinates co-ordinated to a transition metal.[14] There have been a number of reports of the insertion of acetonitrile into M-PR_2 bonds, generating phosphorus analogues of *N*,*N*-dialkylamidinates.[15] In comparison to reported examples of insertion of isocyanides, RNC, into M-C bonds,[16,17] their insertion into M–NR_2 bonds to give metalla-amidinides or η^2-iminocarbamoyls, η^2-RNCNR_2, is also less well explored.[16,18]

The relationship between dicarbollide complexes, [*closo*-3,1,2-M$C_2B_9H_{11}$], and cyclopentadienyl complexes, M(η-C_5H_5), both examples of (Π_2)M complexes,[19] has been discussed in detail elsewhere.[20] In the dicarbollide ligand the two π-donor orbitals are non-degenerate, so it is classified as Π_2', resulting in an orientational preference, often described as a strong *trans* influence of the dicarbollide ligand, as observed in indenyl,[21,22] pyrrolyl[23] and carbonyl[24] complexes. The most widely studied dicarbollide ligand is that derived from *ortho*-carborane, generating [*closo*-3,1,2-M$C_2B_9H_{11}$] complexes.

Here we report the reactions of [*closo*-3,1,2-Ta(NMe_2)$_3$-($C_2B_9H_{11}$)] **2** with nitriles and isocyanides, which proceed by insertion, and with phenol and benzenethiol, which proceed by amminolysis.

Results and discussion

Acetonitrile inserts into the Ta–N bonds of [*closo*-3,1,2-Ta(NMe_2)$_3$($C_2B_9H_{11}$)], **2**, on heating, giving a deep red solution from which pale yellow crystals of the tris-insertion product [*closo*-3,1,2-Ta{N=C(Me)NMe_2}$_3$($C_2B_9H_{11}$)], **3**, were obtained (Scheme 1). The red coloration is thought to be due to the formation of trace poly(acetonitrile). The NMR spectra of **3** are complicated by dynamic exchange processes that are close to coalescence at ambient temperature. The ^{11}B-{^{1}H} NMR spectrum displays 5 B–H resonances in a 1:2:2:3:1 intensity

† Dedicated to the memory of Ron Snaith, a pioneer in the chemistry of *N*,*N*-dialkylamidinates.

Electronic supplementary information (ESI) available: rotatable 3-D crystal structure diagram in CHIME format. See http://www.rsc.org/suppdata/dt/b0/b004862n/

 DOI: 10.1039/b004862n

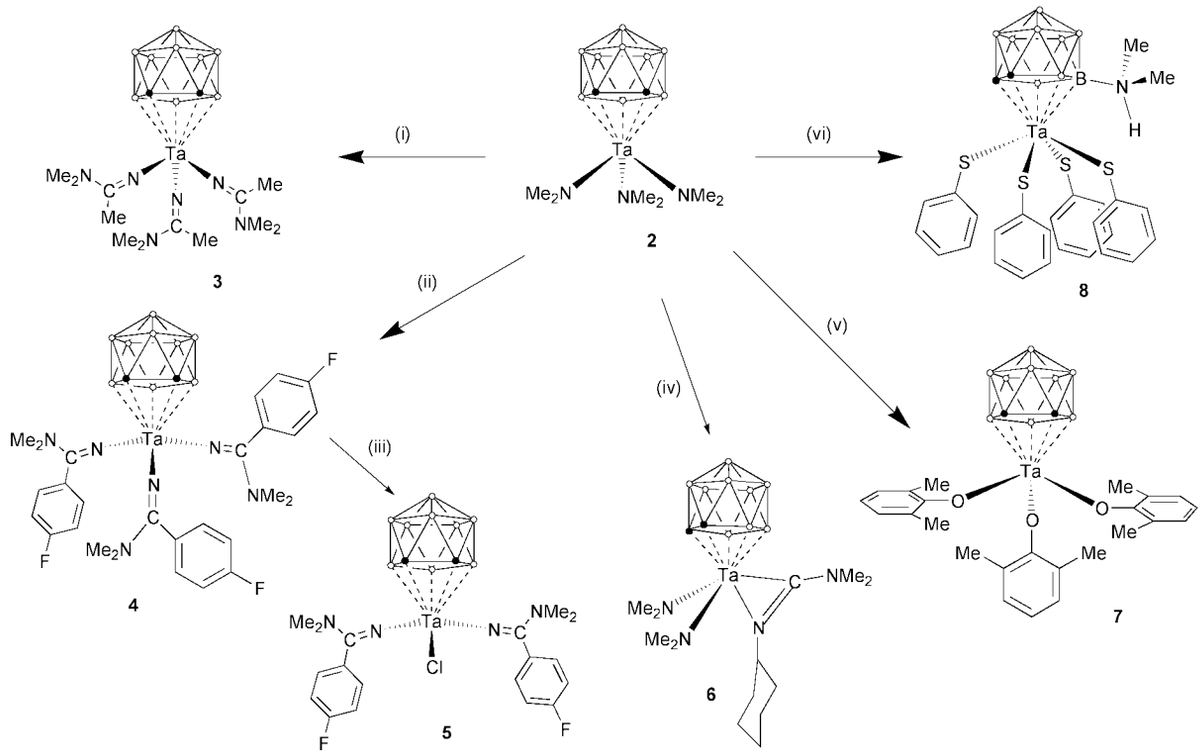

Scheme 1 The reactions of [*closo*-3,1,2-Ta(NMe_2)$_3$($C_2B_9H_{11}$)], **2**, with N=C multiple bonds and with phenol and benzenethiol. Reagents: (i) acetonitrile; (ii) *p*-fluorobenzonitrile; (iii) CH_2Cl_2; (iv) cyclohexyl isocyanide; (v) 2,6-dimethylphenol; (vi) benzenethiol. Filled circles represent cluster CH, open circles cluster BH units.

ratio. The ambient temperature 500 MHz ^{1}H and 125 MHz ^{13}C NMR spectra reveal two NC(Me)NMe_2 ligand environments in a 2 : 1 ratio, with two C–Me resonances in a 2 : 1 ratio. Restricted rotation about the C–NMe_2 bond results in four NMe resonances in a 1 : 1 : 2 : 2 ratio. The 300 MHz ^{1}H and 75 MHz ^{13}C spectra are broadened by the onset of coalescence for rotation about the C–NMe_2 bond. The ^{1}H NMR spectra also show a single broad resonance for the cage C–H hydrogens; the associated ^{13}C resonance is obscured by the solvent, but was located in a HETCOR (heteronuclear correlation) experiment. The related uranium amidinate complexes [U(COT)(N=C(Me)-NEt_2)(THF)$_2$][BPh_4][25] and [U(C_5H_5)$_2${NC(Me)NMe_2}(THF)]-[BPh_4][26] have inequivalent NR_2 groups due to restricted rotation around the C–NR_2 bond in the ligands.

The reaction of compound **2** with *p*-fluorobenzonitrile, N≡CC_6H_4F, gives [*closo*-3,1,2-Ta{N=C(C_6H_4F)NMe_2}$_3$(C_2B_9-H_{11})] **4** which may be isolated as a bright yellow powder, and purified by crystallisation from hot toluene, in which it is sparingly soluble. The poor solubility of **4** in solvents with which it does not react has hampered satisfactory spectroscopic characterisation. Attempted re-crystallisation by diffusion of pentane into a solution of **4** in dichloromethane gives colourless crystals of [*closo*-3,1,2-Ta{N=C(C_6H_4F)NMe_2}$_2$Cl(C_2B_9-H_{11})], **5**, where one amidinate ligand has been replaced by a chloride. Dehydrochlorination reactions have been observed in other areas of main group[27] and transition metal amide chemistry,[28] and arise from the high basicity and polar nature of the M–N bond.[29] The 400 MHz ^{1}H-{^{11}B} and 100 MHz ^{13}C NMR spectra of **5** reveal the presence of two cage C–H signals and a total of 8 B–H signals in a 1 : 1 : 1 : 1 : 2 : 1 : 1 ratio. The 9th B–H resonance could not be observed in the ^{1}H-{^{11}B} NMR spectrum, intensity ratios suggest that this signal is hidden under the methyl group signals. The ^{1}H NMR spectrum also shows resonances assigned to two different NMe_2 groups in a 1 : 1 ratio. This observation of two similar ligand environments in a 1 : 1 ratio is repeated for the remaining signals in both the ^{1}H and ^{13}C NMR spectra. The ^{13}C NMR spectrum shows 4 signals assigned to the phenyl groups, indicating free rotation about the NC–C_6H_4F bond in two inequivalent ligands. Assignment of the ^{13}C NMR spectrum was assisted by comparison of the C-F coupling constants with those of the starting nitrile, *p*-fluorobenzonitrile. The ^{19}F (188 MHz) NMR spectrum shows two ^{19}F environments in a 1 : 1 intensity ratio.

The reaction of compound **2** with three equivalents of cyclohexyl isocyanide yields only the mono-insertion product [Ta(NMe_2)$_2${η^2-N(Cy)CNMe_2}($C_2B_9H_{11}$)], **6**. The ^{11}B-{^{1}H} NMR spectrum of **6** shows 5 resonances in a 1 : 3 : 2 : 1 : 2 intensity ratio indicating a C_s symmetrical molecule. The ^{1}H and ^{13}C NMR spectra show only one resonance for the C–H unit in the cage, confirming the symmetry. The ^{1}H NMR spectrum also shows the presence of three N–Me groups in a 4 : 1 : 1 intensity ratio, which is also seen in the ^{13}C NMR spectrum, and a series of C–H multiplets with a total integral of 11 H, assigned to the cyclohexyl group. The *C*H_3, *C*H_2 and *C*H units were identified by ^{13}C DEPT experiments. One geometry consistent with these data for **6** is shown in Scheme 1, with free rotation about the Ta–NMe_2 bonds in solution at room temperature and the N(Cy)CNMe_2 ligand lying in the molecular mirror plane, with two inequivalent N–Me groups also in the mirror plane. The available spectroscopic data cannot exclude the alternative structure with the N–Cy group adjacent to the cage, or a fluxional structure of lower symmetry. We have been unable to grow suitable crystals for a structural study.

Since only starting materials were recovered from refluxing toluene solutions of compound **2** with the carbon-based acids C_5H_6, C_5H_5Me or phenylacetylene,[6] the reactions of **2** with co-ordinating acids, which are kinetically more reactive, were next investigated. The reaction with four equivalents of 2,6-dimethylphenol in toluene solution at 80 °C yields colourless [*closo*-3,1,2-Ta($OC_6H_3Me_2$-2,6)$_3$($C_2B_9H_{11}$)], **7**. Attempts to treat **2** with stoichiometric quantities of methanol or ethanol resulted in the formation of [NH_2Me_2][*nido*-$C_2B_9H_{12}$]. The ^{11}B-{^{1}H} NMR spectrum of **7** shows 5 resonances in a 1 : 2 : 2 : 3 : 1 intensity ratio. The ^{1}H NMR spectrum confirms the molecular C_s symmetry of the molecule in solution with the presence of only one cage C–*H* resonance. The ^{13}C and ^{1}H

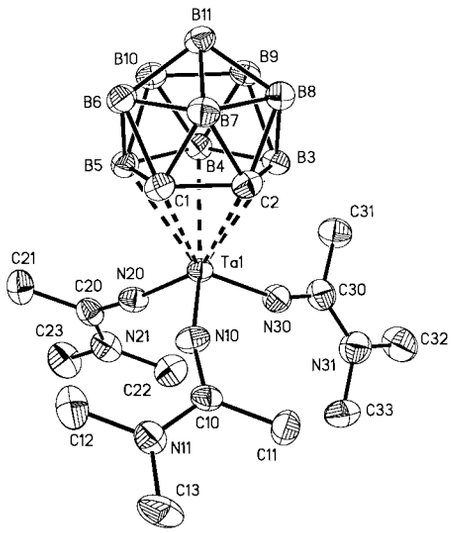

Fig. 1 The molecular strucuture of [*closo*-3,1,2-Ta{N=C(Me)NMe_2}$_3$-($C_2B_9H_{11}$)] **3** showing 50% displacement ellipsoids. Hydrogen atoms have been omitted for clarity.

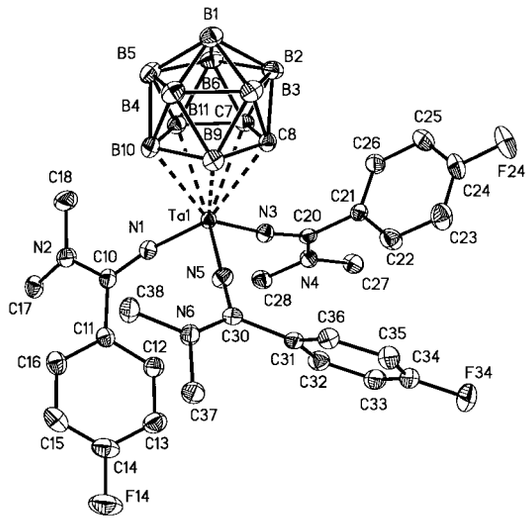

Fig. 2 The molecular structure of [*closo*-3,1,2-Ta{N=C(C_6H_4F)-NMe_2}$_3$($C_2B_9H_{11}$)] **4**. Details as in Fig. 1.

NMR spectra also show only one methyl environment and one *meta* environment in the aromatic ring, consistent with rapid rotation around the metal–oxygen bond, and exchange of the "vertical" and "horizontal" phenoxide ligands. Attempts to freeze out the these processes in variable temperature NMR experiments, by cooling a sample of **7** in CD_2Cl_2 to −90 °C, proved unsuccessful, showing no decoalescence.

The reaction of 4 equivalents of benzenethiol with compound **2** produces red needle-like crystals of the charge-compensated[30] complex [*closo*-3-Ta(SC_6H_5)$_4$(9-$NHMe_2$-1,2-$C_2B_9H_{10}$)], **8**, where the β-boron of the C_2B_3 face bears a $NHMe_2^+$ substituent. The ^{11}B NMR spectrum of **8** shows 5 doublets and one singlet resonance in a 1:2:2:2:1:1 intensity ratio, with the low frequency singlet at δ 23.3 corresponding to the boron to which the $NHMe_2$ is co-ordinated. The ^{1}H NMR spectrum shows the cage to be symmetrical with one resonance for the cage C–H at δ 3.19. The N–CH_3 protons are clearly identified, as is the resonance for the hydrogen on the NMe_2 group attached to the cage. The phenyl region of the spectrum shows a series of multiplets that integrate to 20 H; this region of the spectrum along with the 4 resonances observed in the ^{13}C-{^{1}H} spectrum indicates free rotation of the SPh groups.

The mechanism by which compound **8** is formed is not known but the reaction is reproducible and the product may be isolated in a moderate yield, 53%. There are many reports in the literature in which charge-compensated carborane ligands have been prepared, using various methods including ligand rearrangement from metal site to the carborane cage,[31] nucleophilic substitution,[32] reduction of a metallacarborane complex by a Lewis base,[33] and addition of dialkyl sulfide to a protonated metallocene-type sandwich complex.[34] Amine substituted dicarbollide systems, where the amine has substituted the hydrogen atom at the unique boron in the C_2B_3 face, have been prepared by the $FeCl_3$-promoted oxidative coupling of *nido*-7,8-$C_2B_9H_{12}$ salts with amines such as triethylamine.[35] It is possible that the benzenethiol contained a quantity of diphenyl disulfide, PhSSPh, which reacts with the dicarbollide cage of [Ta(SPh)$_3$($C_2B_9H_{11}$)] to form the cationic intermediate [Ta(SPh)$_3$(9-PhS-$C_2B_9H_{11}$)]$^+$, which in turn is attacked by free Me_2NH giving **8**.

Crystallography

The molecular structure of the acetonitrile insertion product, [*closo*-3,1,2-Ta{N=C(Me)NMe_2}$_3$($C_2B_9H_{11}$)] **3** is shown in Fig. 1 and selected bond lengths and angles are given in Table 1, whilst the *p*-fluorobenzonitrile insertion product [*closo*-3,1,2-Ta{N=C(C_6H_4F)NMe_2}$_3$($C_2B_9H_{11}$)] **4**, which crystallises with a half molecule of benzene solvate, is shown in Fig. 2 and selected bond lengths and angles are also given in Table 1. The *N*,*N*-dimethylamidinate ligands in both **3** (*N*,*N*-dimethylacetamidinate) and **4** (*p*-fluoro-*N*,*N*-dimethylbenzamidinate) are co-ordinated in a monodentate fashion, giving an approximate propeller-like geometry to the TaL_3 unit, with one ligand localised *cis* to the C_2 unit of the $C_2B_9H_{11}$ ligand.

In compound **3** the *N*,*N*-dimethylacetamidinate ligands are close to planar, with mean deviations from planarity of the Ta–N–C–(C)–NC_2 units varying from 0.033 Å for the ligands containing N(20) and N(30) to 0.074 Å for the ligand containing N(10) which lies *cis* to the C_2 unit of the cage. The ligand containing N(10) has the NMe_2 unit on the cage side of the N(10)–N(20)–N(30) plane, with the former acetonitrile methyl group directed away from the cage; the situation is reversed in the other two ligands. The angles between the centroid–Ta–N planes and the acetamidinate ligand planes are 80.5 N(10), 144.0 N(20) and 140.6° N(30) so that the unique acetamidinate ligand, containing N(10), is more nearly parallel to the C_2B_3 face of the cage than the other two. The longest Ta–N bond is to the ligand containing N(10) and the Ta–N distances are intermediate between typical amide Ta–NR_2 distances (CSD mean 1.99 Å; 1.949(4) to 1.987(5) Å in **2**),[36] and tantalum imido Ta–NR distances (CSD 1.75 to 1.82 Å, mean 1.79 Å). Finally, the N–C bonds in the amidinate are shorter than typical N–C single bonds.

In compound **4**, the Ta–N–C–(C_{ipso})–NC_2 units are also close to planar, with mean deviations from planarity of 0.002 (N2), 0.036 (N5) and 0.067 Å (N1), although the *p*-fluorophenyl fragments are twisted out of these planes. The angles between the centroid–Ta–N planes and the amidinate ligand planes are 34.0 N(1), 42.3 N(3) and 99.2° N(5), so that the ligand containing N(5) is more nearly parallel with the C_2B_3 face of the cage. The ligand containing N(3) has its phenyl group on the cage side of the N(1)–N(3)–N(5) plane, whilst the other two ligands have the NMe_2 group on the cage side of this plane.

These structural features of compounds **3** and **4** reflect a delocalised π-bonding framework over the entire amidinate ligand and a balance between the two canonical forms, (I) tantalum amide and (II) tantalum imide. The strong π donation to the metal atom from three amidinate ligands results in a

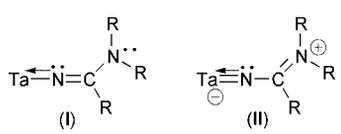

Table 1 Selected bond lengths (Å) and angles (°) for [*closo*-3,1,2-Ta{N=CMe(NMe_2)}$_3$($C_2B_9H_{11}$)] **3**, [*closo*-3,1,2-Ta{N=C(C_6H_4F)NMe_2}$_3$($C_2B_9H_{11}$)] **4** and [*closo*-3,1,2-Ta{N=C(C_6H_4F)NMe_2}$_2$Cl($C_2B_9H_{11}$)] **5**

3		**4**		**5**	
Ta(1)–N(10)	1.922(3)	Ta(1)–N(1)	1.9125(16)	Ta(1)–N(1)	1.870(3)
Ta(1)–N(20)	1.878(3)	Ta(1)–N(3)	1.9049(16)	Ta(1)–N(3)	1.859(3)
Ta(1)–N(30)	1.912(4)	Ta(1)–N(5)	1.8863(16)	Ta(1)–Cl(1)	2.397(1)
Ta(1)–C(1)	2.589(4)	Ta(1)–C(7)	2.526(2)	Ta(1)–C(7)	2.479(4)
Ta(1)–C(2)	2.619(4)	Ta(1)–C(8)	2.568(2)	Ta(1)–C(8)	2.501(3)
Ta(1)–B(3)	2.547(4)	Ta(1)–B(9)	2.548(2)	Ta(1)–B(9)	2.499(4)
Ta(1)–B(4)	2.460(4)	Ta(1)–B(10)	2.487(2)	Ta(1)–B(10)	2.461(4)
Ta(1)–B(5)	2.460(4)	Ta(1)–B(11)	2.466(2)	Ta(1)–B(11)	2.462(4)
Ta(1)–Cb	2.097(5)	Ta(1)–Cb	2.068(3)	Ta(1)–Cb	2.018(5)
N(10)–C(10)	1.279(5)	N(1)–C(10)	1.286(2)	N(1)–C(10)	1.297(5)
N(20)–C(20)	1.303(6)	N(3)–C(20)	1.288(2)	N(3)–C(20)	1.304(4)
N(30)–C(30)	1.314(6)	N(5)–C(30)	1.291(2)		
C(10)–N(11)	1.348(6)	C(10)–N(2)	1.365(3)	C(10)–N(2)	1.337(5)
C(20)–N(21)	1.336(6)	C(20)–N(4)	1.347(2)	C(20)–N(4)	1.328(5)
C(30)–N(31)	1.344(7)	C(30)–N(6)	1.347(2)		
Cb–Ta(1)–N(10)	106.4(2)	Cb–Ta(1)–N(1)	124.3(2)	Cb–Ta(1)–N(1)	116.7(3)
Cb–Ta(1)–N(20)	124.1(2)	Cb–Ta(1)–N(3)	113.1(2)	Cb–Ta(1)–N(3)	123.5(2)
Cb–Ta(1)–N(30)	118.4(2)	Cb–Ta(1)–N(5)	113.5(2)	Cb–Ta(1)–Cl(1)	112.2(1)
Ta(1)–N(10)–C(10)	161.3(3)	Ta(1)–N(1)–C(10)	162.8(2)	Ta(1)–N(1)–C(10)	168.1(3)
Ta(1)–N(20)–C(20)	173.7(3)	Ta(1)–N(3)–C(20)	167.2(2)	Ta(1)–N(3)–C(20)	172.7(3)
Ta(1)–N(30)–C(30)	157.7(7)	Ta(1)–N(5)–C(30)	174.5(2)		

Cb = Centroid of the η^5-co-ordinated C_2B_3 ring.

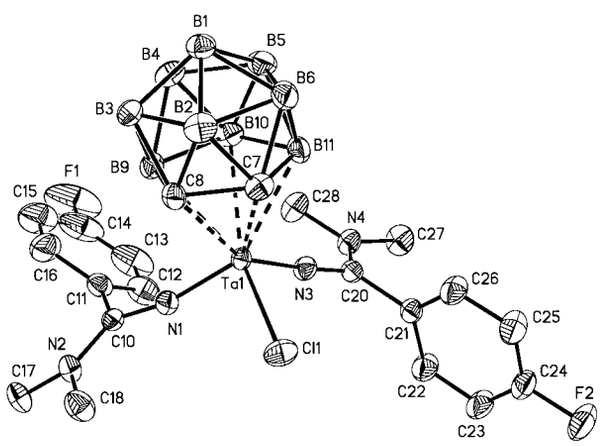

Fig. 3 The molecular structure of [*closo*-3,1,2-Ta{N=C(C_6H_4F)-NMe_2}$_2$Cl($C_2B_9H_{11}$)] **5**. Details as in Fig. 1.

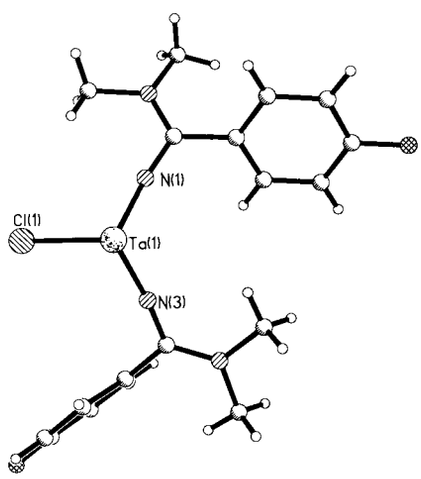

Fig. 4 A view orthogonal to the ligand plane of the Ta{N=C-(C_6H_4F)NMe_2}$_2$Cl fragment of compound **5**. Hydrogen atoms have been omitted for clarity.

competitive weakening of the carborane to metal π donation, and complex **3** shows the longest centroid–metal distance seen in the present study.

In the solid state each molecule of [*closo*-3,1,2-Ta{N=C(C_6-H_4F)NMe_2}$_2$Cl($C_2B_9H_{11}$)], **5**, is accompanied by two independent molecules of dichloromethane; the molecular structure is shown in Fig. 3, and selected bond lengths and angles appear in Table 1. Each *p*-fluoro-*N*,*N*-dimethylbenzamidinate ligand is co-ordinated to the tantalum in a monodentate fashion, with slightly different Ta–N bond distances (1.870(3) and 1.859(3) Å), which are shorter than those in **3**. As in **3**, the amidinate ligand is very close to planar, with the *p*-fluorophenyl group out of plane. The partial multiple character of both Ta–N and N–C bonds prevents rotation about them, and results in two inequivalent *p*-fluorophenyl groups, *cis* and *trans* respectively with respect to the Ta-Cl bond (Fig. 4), as evidenced by the NMR data. The carbon atom positions in the dicarbollide cage are clearly identified, with the Ta–Cl bond lying directly beneath the cage carbon atom C(7). The Ta–Cl bond in **5** is longer than in [$TaCl_3(C_2B_9H_{11})$] (2.205(5) to 2.259(5) Å),[2] as a consequence of the steric bulk of the two amidinate ligands, and a reduction in the Lewis acidity of the Ta atom.

In the solid state the asymmetric unit of [*closo*-3,1,2-Ta($OC_6H_3Me_2$-2,6)$_3$($C_2B_9H_{11}$)], **7**, comprises two molecules, A and B, with similar geometries (Fig. 5 shows molecule A and data for both are given in Table 2). The tantalum atom is co-ordinated by the open C_2B_3 face of the dicarbollide ligand (in a nearly symmetrical η^5 fashion) and by three dimethylphenoxide ligands. This complex exhibits evidence of the *trans* influence of the dicarbollide ligand, with two phenoxide ligands lying nearly parallel to the C_2B_3 face, and one perpendicular, in a fashion reminiscent of the structure of [$Ta(NMe_2)_3(C_2B_9$-$H_{11})$] and [$Nb(S_2NMe_2)_3(C_2B_9H_{11})$].[1] A similar orientation of alkoxide ligands is observed in [Ti(^{t}Bu)($OC_6H_3{}^i$Pr$_2$-2,6)$_3$].[37] The carbon atoms in the C_2B_3 face were clearly identified in both molecules, with one carbon atom lying almost directly *trans* to the unique phenoxide ligand. This results in a pseudo mirror symmetry which is only violated by the non-equivalence of C(8) and B(11) in molecule A and C(78) and B(81) in molecule B.

The planes defined by the C_2B_3 face of the dicarbollide ligand and the three oxygen atoms of the phenoxide ligands are not exactly parallel, with angles between the two planes of 2.6 and 1.8° in molecule A and B respectively. The dicarbollide ligand tilts forward, away from the unique phenoxide ligand. The Ta–O bond to the unique phenoxide ligand is shorter than to

the other two, and shows a larger centroid–Ta–O angle, *i.e*. the oxygen moves away from the cage to reduce steric interaction and the cage tilts forward also to relieve interaction between the phenoxide ligand and B–H bonds.

In the solid state [*closo*-3-Ta(SC_6H_5)$_4$(9-$NHMe_2$-1,2-$C_2B_9H_{10}$)], **8**, co-crystallises with one molecule of disordered toluene; the molecular structure of **8** appears in Fig. 6 and selected bond lengths and angles are given in Table 3. The Ta(SPh)$_4$ fragment has a distorted four-legged piano-stool structure, with approximate molecular C_2 symmetry (Fig. 7). The thiolate ligands containing S(1) and S(3) are bent away from the dicarbollide ligand (centroid–Ta–S angles of 123.3(3) and 119.1(3)° respectively), whilst the thiolate ligands containing S(2) and S(4) are displaced towards the dicarbollide ligand and do not have such pronounced angles at tantalum (centroid–Ta–S angles of 106.0(3) and 104.0(3)° respectively). The planes of the phenyl groups on S(1) and S(3) are almost co-parallel, but point in opposite directions, with an angle between the two planes of 2.5°, whilst the phenyl groups on S(2) and S(4) have a much greater angle (140.0°) between them. This ligand orientation differs from that observed in the related structure of [Ta($C_5H_4CH_3$)(SC_6H_5)$_4$],[38] where two of the phenyl groups are almost perpendicular to each other.

The Ta–S(3) distance is slightly shorter than the other three Ta–S distances, although all are in the range of typical tantalum(v)–thiolate distances, 2.35–2.47 Å.[39,40] The Ta–centroid distance is slightly longer than those observed in other tantalum dicarbollide species, 1.963(3)–2.028(4) Å. This is not unexpected as the SPh groups are very good donor groups to the metal, resulting in a weakening of the M–cluster bonding interaction, and the [*nido*-10-$NHMe_2$-7,8-$C_2B_9H_{11}$]$^-$ ligand is a mono- rather than di-anionic ligand.

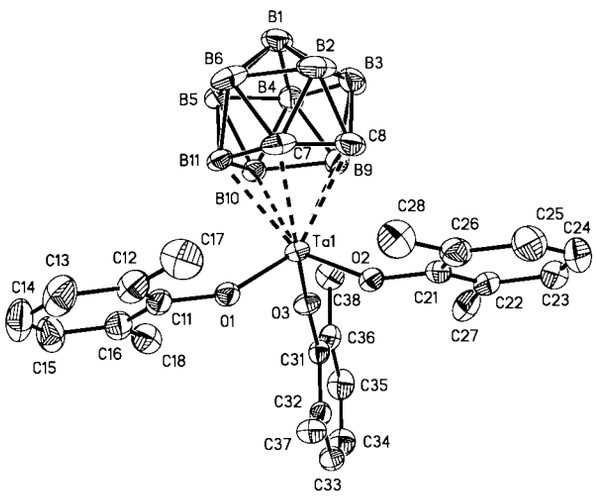

Fig. 5 The molecular structure of [*closo*-3,1,2-Ta($OC_6H_3Me_2$-2,6)$_3$-($C_2B_9H_{11}$)], **7**. Only molecule A is shown. Other details as in Fig. 1.

Table 2 Selected bond lengths (Å) and angles (°) for [*closo*-3,1,2-Ta($OC_6H_3Me_2$-2,6)$_3$($C_2B_9H_{11}$], **7**

	Molecule A		Molecule B
Ta(1)–C(7)	2.462(3)	Ta(2)–C(77)	2.483(3)
Ta(1)–C(8)	2.447(3)	Ta(2)–C(78)	2.428(3)
Ta(1)–B(9)	2.400(3)	Ta(2)–B(79)	2.409(3)
Ta(1)–B(10)	2.408(3)	Ta(2)–B(80)	2.413(3)
Ta(1)–B(11)	2.443(3)	Ta(2)–B(81)	2.449(3)
Cb–Ta(1)	1.963(3)	Cb–Ta(2)	1.956(3)
C(7)–C(8)	1.612(5)	C(77)–C(78)	1.638(4)
Ta(1)–O(1)	1.878(2)	Ta(2)–O(4)	1.853(2)
Ta(1)–O(2)	1.880(2)	Ta(2)–O(5)	1.882(2)
Ta(1)–O(3)	1.844(2)	Ta(2)–O(6)	1.857(2)
Ta(1)–O(1)–C(11)	153.0(2)	Ta(2)–O(4)–C(41)	160.5(2)
Ta(1)–O(2)–C(21)	151.0(2)	Ta(2)–O(5)–C(51)	153.2(2)
Ta(1)–O(3)–C(31)	165.0(2)	Ta(2)–O(6)–C(61)	164.4(2)

Cb = Centroid of the η^5-co-ordinated C_2B_3 ring.

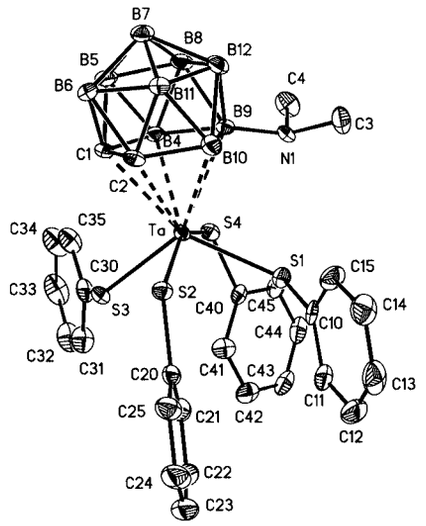

Fig. 6 The molecular structure of [*closo*-3-Ta(SC_6H_5)$_4$(9-$NHMe_2$-1,2-$C_2B_9H_{10}$)], **8**. Details as in Fig. 1.

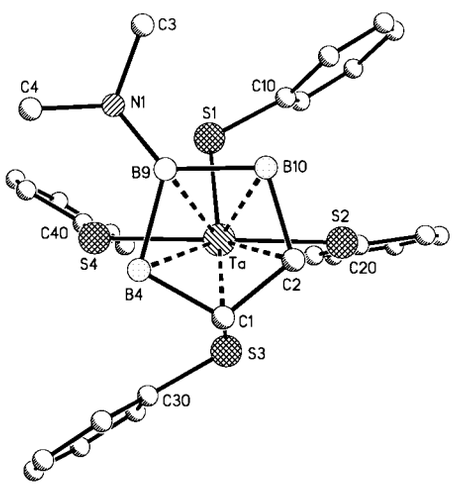

Fig. 7 A view of compound **8** along the molecular pseudo-twofold axis, showing the approximate C_2 symmetry of the Ta(SPh)$_4$ unit, and the alternating arrangement of the SPh ligands. Hydrogen atoms have been omitted for clarity.

Table 3 Selected bond lengths (Å) and angles (°) for [*closo*-3-Ta(SPh)$_4$(9-$NHMe_2$-1,2-$C_2B_9H_{10}$)], **8**

Ta–C(1)	2.515(6)	Ta–C(2)	2.456(6)	C(1)–C(2)	1.573(8)
Ta–B(4)	2.539(6)	Ta–B(9)	2.552(6)	Ta–B(10)	2.489(7)
Ta–Cb	2.053(6)				
Ta–S(1)	2.4255(14)	Cb–Ta–S(1)	123.3(3)	Cb–Ta–S(1)–C(10)	90.0(3)
Ta–S(2)	2.4224(14)	Cb–Ta–S(2)	106.0(3)	Cb–Ta–S(2)–C(20)	180.0(3)
Ta–S(3)	2.4177(14)	Cb–Ta–S(3)	119.1(3)	Cb–Ta–S(3)–C(30)	83.9(4)
Ta–S(4)	2.4580(16)	Cb–Ta–S(4)	104.0(3)	Cb–Ta–S(4)–C(40)	167.9(4)

Cb = Centroid of the η^5-co-ordinated C_2B_3 ring.

Extended Hückel molecular orbital studies on $[Ta(C_5H_5)(SH)_4]$, as a model for $[Ta(C_5H_4CH_3)(SC_6H_5)_4]$,[38] show that π bonding between the sulfur π-donor orbitals and the d_{x^2} and d_{xy} orbitals accounts for most of the observed centroid–Ta–S angles, *i.e.* S(1) and S(3) are shifted down to maximise overlap with the d_{x^2} orbital, while S(2) and S(4) are displaced towards the Cp ligand to maximise overlap with the d_{xy} orbital. The d_{xz} and d_{yz} orbitals which are Ta–Cp bonding appear to contribute significantly to the M–L σ bonding in $CpML_4$ compounds.[41] The substituted dicarbollide ligand [*nido*-10-$NHMe_2$-7,8-$C_2B_9H_{11}]^-$ in **8** has the same overall charge and very similar frontier orbitals to the $[C_5H_5]^-$ ligand, and it is likely that the electronic structures of $[Ta(C_5H_4CH_3)(SC_6H_5)_4]$ and **8** are similar.

The orientation of the $NHMe_2$ unit is of some interest, as it lies between S(1) and S(4), with the hydrogen atom pointing down into the plane of the sulfur atoms. Although the distances H(1N)···S(1) and H(1N)···S(4) are 2.78 and 2.67 Å respectively and direct hydrogen bonding can be ruled out, some weaker form of electrostatic interaction may be responsible for the directionality of the N(1)–H(1N) bond. The angle N(1)–B(9)–centroid is 160.7° and not dissimilar from the H–B–centroid angle at the unsubstituted cage boron atoms.

Experimental

All manipulations of air- and moisture-sensitive compounds were performed on a conventional vacuum/nitrogen line using standard Schlenk and cannula techniques or in a nitrogen filled glove box. When required, solvents were dried by prolonged reflux over an appropriate drying agent prior to distillation and deoxygenation by freeze–pump–thaw processes. NMR solvents were vacuum-distilled from suitable drying agents and stored in ampoules under a dry nitrogen atmosphere. Elemental analysis was performed by the micro-analytical service within this department. Infrared spectra were run as liquid films on a Perkin-Elmer 1615 FTIR spectrometer or as solid samples on a Graseby Specac 10500 Golden Gate coupled to a Perkin-Elmer 1000 series "Paragon" spectrometer, mass spectra on a Micromass Autospec instrument operating in EI mode (in each case the highest abundance peak in the envelope is quoted). NMR spectra were recorded on the following instruments: Varian Gemini-200 (^{19}F); Varian Unity-300 (^1H, ^{11}B, ^{13}C); Varian VXR-400 (^1H, ^{13}C); Varian 500 (^1H, ^{13}C and HETCOR); ^1H and ^{13}C spectra on the Unity-300 unless otherwise stated. All chemical shifts are reported in δ (ppm) and coupling constants in Hz. ^1H NMR spectra were referenced to residual protio impurity in the solvent (C_6D_5H, δ 7.15; $CHCl_3$, 7.26; $CDHCl_2$, 5.25), ^{13}C to the solvent resonance (C_6D_6, δ 128.0; $CDCl_3$, 77.0; CD_2Cl_2, 53.5) and ^{19}F and ^{11}B externally to $CFCl_3$, and $BF_3{\cdot}Et_2O$ respectively, δ 0. Except where otherwise indicated, all spectra were recorded at ambient temperature.

Syntheses

[*closo*-3,1,2-Ta{N=C(Me)NMe_2}$_3$($C_2B_9H_{11}$)] 3. In a Young's ampoule a stirred toluene (20 cm^3) solution of compound **2** (0.445 g, 1 mmol) was treated dropwise with $NCMe_3$ (0.143 g, 3.5 mmol). The ampoule was evacuated and the solution heated to 130 °C and maintained at this temperature for 48 h. The reaction mixture slowly changed from pale yellow to deep red. It was allowed to cool to room temperature and the solvent evaporated under reduced pressure. The orange residue was extracted with dichloromethane (10 cm^3) and layered with pentane (10 cm^3), which produced a pale yellow powder that was isolated by careful filtration. This process was repeated two times and resulted in the isolation of a pale yellow microcrystalline precipitate. Yield 0.22 g, 39%. ^1H NMR (500 MHz, CD_2Cl_2): δ 3.20 (s, 3 H, NMe) 3.12 (s, 6 H, 2 × NMe), 3.06 (s, 6 H, 2 × NMe), 3.04 (s, 3 H, NMe) 2.90 (s, 2 H, carborane C–H), 2.31 (s, 3 H, C–Me) and 2.21 (s, 6 H, C–Me). Additional peaks in ^1H-{^{11}B} NMR (CD_2Cl_2): δ 2.77 (1 H), 2.14 (2 H), 2.02 (2 H), 1.85 (1 H) and 1.69 (3 H). ^{13}C-{^1H} NMR (125 MHz, CD_2Cl_2) assigned by HETCOR: δ 169.9 (1 × N=*C*(Me)NMe_2), 163.8 (2 × N=*C*(Me)NMe_2), 54.2 (carborane CH), 39.4, (1 × C–N*Me*) 39.3 (1 × C–N*Me*), 38.9 (C–N*Me*$_2$), 38.5 (C–N*Me*$_2$), 21.8 (2 × N=C–*Me*) and 17.7 (1 × N=C–*Me*). ^{11}B NMR ($CDCl_3$): δ −0.5 (d, 1B, J_{B-H} 108), −4.9 (d, 2B, J_{B-H} 138), −8.1 (d, 2B, J_{B-H} 99), −13.4 (d, 3B, J_{B-H} 153) and −17.4 (d, 1B, J_{B-H} 144 Hz). Calc. for $C_{14}H_{38}B_9N_6Ta$: C, 29.57; H, 6.73; N, 14.78. Found: C, 29.55; H, 6.91; N, 14.06%. MS: *m/z* 569 [M^+], 484 [M^+ − (NC(Me)NMe_2)] and 436 [$M^+ - C_2B_9H_{11}$].

[*closo*-3,1,2-Ta{NC(C_6H_4F)NMe_2}$_3$($C_2B_9H_{11}$)] 4. In a Young's ampoule a stirred toluene (10 cm^3) solution of compound **2** (0.445 g, 1 mmol) was treated dropwise with a toluene solution (10 cm^3) of NCC_6H_4F-*p* (0.42 g, 3.5 mmol). The ampoule was evacuated and the solution heated to 130 °C and maintained at this temperature for 48 h. The reaction mixture slowly changed from pale yellow to deep red. It was then allowed to cool to room temperature and the solvent evaporated under reduced pressure. The residue was extracted with hot toluene, filtered and allowed to cool to room temperature, when bright yellow [*closo*-3,1,2-Ta{NC(C_6H_4F)NMe_2}$_3$($C_2B_9H_{11}$)] **4** precipitated. Crystals suitable for X-ray diffraction were grown by sealing a small amount of material in a 5 mm NMR tube containing benzene-d_6, heating to 60 °C and allowing to cool slowly to room temperature. ^1H NMR (300 MHz, C_6D_6): δ 7.07–6.56 (m, 12 H, C_6H_4), 4.53 (br s, 2 H, carborane CH), 2.64 (s, 12 H, NMe) and 2.57 (s, 6 H, NMe). ^{11}B NMR (96.2 MHz, C_6D_6): δ 5.1 (2B), −0.2 (3B), −4.9 (2B), −10.6 (1B) and −14.1 (1B). Calc. for $C_{29}H_{41}B_9F_3N_6Ta{\cdot}0.25C_6H_6$: C, 44.2; H, 5.2; N, 10.1. Found: C, 44.1; H, 5.2; N, 9.5%.

[*closo*-3,1,2-Ta{N=C(C_6H_4F)NMe_2}$_2$Cl($C_2B_9H_{11}$)] 5. The initial stages of the synthesis of compound **4** were followed. The red/orange residue from the reaction was extracted with dichloromethane (10 cm^3) and layered with pentane (10 cm^3), which produced a pale yellow powder that was isolated by careful filtration. This process was repeated two times and resulted in the isolation of a yellow microcrystalline precipitate. Slow recrystallisation from a concentrated dichloromethane solution layered with pentane at −20 °C formed crystals suitable for single crystal X-ray diffraction experiments. Yield 0.33 g, 49%. ^1H NMR (400 MHz, CD_2Cl_2): δ 3.10 (s, 1 H, carborane C–H), 3.32 (s, 1 H, carborane C–H), 3.00 (s, 6 H, NMe_2), 3.20 (s, 6 H, NMe_2) and 6.98–7.5 (M, 8 H, 2 × C_6H_4F). Additional peaks in ^1H-{^{11}B} NMR (300 MHz, CD_2Cl_2): δ 1.50 (1 H), 1.58 (1 H), 1.80 (1 H), 1.99 (1 H), 2.06 (2 H), 2.32 (1 H) and 2.75 (1 H); 9th B–H hidden under C–H and NMe region. ^{19}F NMR (188 MHz, CD_2Cl_2): δ −107.15 (s, 1F) and −110.06 (s, 1F). ^{13}C-{^1H} NMR (100.57 MHz, CD_2Cl_2): δ 39.5 (NMe_2), 40.7 (br, $C_2B_9H_{11}$), 41.7 (NMe_2), 42.5 (br, $C_2B_9H_{11}$), 115.7 (d, *ortho*-C of C_6H_4F, J_{C-F} 22), 116.8 (d, *ortho*-C of C_6H_4F, J_{C-F} 23), 128.4 (s, N=C), 129.2 (s, N=C), 130.0 (d, *para*-C of C_6H_4F, J_{C-F} 3), 130.2 (d, *meta*-C of C_6H_4F, J_{C-F} 9), 130.9 (d, *para*-C of C_6H_4F, J_{C-F} 3), 131.2 (d, *meta*-C of C_6H_4F, J_{C-F} 9), 163.6 (d, C–F, J_{C-F} 251) and 165.1 (d, C–F, J_{C-F} 254 Hz). ^{11}B NMR (96.2 MHz, $CDCl_3$): δ 0.7 (d, 1B, J_{B-H} 118), −4.3 (d, 2B, J_{B-H} 141), −7.5 (d, 3B J_{B-H} 130), −13.9 (d, 2B, J_{B-H} 144) and −16.9 (d, 1B, J_{B-H} 139 Hz). Calc. for $C_{20}H_{31}ClB_9F_2N_4Ta{\cdot}1.3CH_2Cl_2$: C, 32.4; H, 4.3; N, 7.1. Found: C, 32.6; H, 4.3, N, 7.2%.

[*closo*-3,1,2-Ta(NMe_2)$_2${η^2-N(Cy)CNMe_2}($C_2B_9H_{11}$)] 6. A stirred toluene (10 cm^3) solution of compound **2** (0.445 g, 1 mmol) was treated dropwise with a toluene solution (10 cm^3) of CNC_6H_{11} (0.35 g, 3.2 mmol). The yellow solution was warmed to 110 °C and maintained at this temperature for 12 h. The reaction mixture was allowed to cool to room temperature and the solvent evaporated under reduced pressure. The orange

Table 4 Crystal data for compounds **3**, **4**, **5**, **7** and **8**

	3	**4**	**5**	**7**	**8**
Formula	$C_{14}H_{38}B_9N_6Ta$	$C_{32}H_{44}B_9F_3N_6Ta$	$C_{22}H_{35}B_9Cl_3F_2N_4Ta$	$C_{26}H_{38}B_9O_3Ta$	$C_{31.5}H_{37}B_9NS_4Ta$
M	568.74	847.97	849.03	676.80	836.10
Crystal system	Triclinic	Monoclinic	Triclinic	Monoclinic	Triclinic
Space group	$P\bar{1}$	$P2_1/c$	$P\bar{1}$	$P2_1/c$	$P\bar{1}$
a/Å	9.3136(5)	13.104(3)	10.122(2)	18.732(3)	11.236(1)
b/Å	10.4888(6)	18.420(4)	12.074(2)	19.920(3)	11.950(1)
c/Å	13.2061(7)	15.495(4)	15.206(3)	15.986(3)	15.081(2)
α/°	78.322(1)		90.21(1)		110.016(3)
β/°	83.674(1)	90.976(4)	105.49(1)	95.108(4)	96.548(2)
γ/°	75.013(1)		104.14(1)		102.996(2)
U/Å^3	1218.12(12)	3739.6(15)	1732.0(6)	5941.4(17)	1813.1(3)
Z	2	4	2	8	2
μ(Mo-Kα)/mm^{-1}	4.525	2.987	3.592	3.727	3.286
Reflections measured	13888	42691	22150	71190	21823
Unique reflections	5565	9287	9387	16897	9807
R(int)	0.0214	0.0304	0.0221	0.0329	0.0864
Reflections with $I \geq 2\sigma(I)$	5000	8380	8767	12834	6099
R [$F^2 > 2\sigma(F^2)$]	0.030	0.018	0.033	0.024	0.050
$wR(F^2)$, all data	0.078	0.047	0.090	0.057	0.090

residue was extracted with fresh toluene (10 cm^3) filtered and carefully layered with pentane (10 cm^3). Slow recrystallisation at −20 °C produced a yellow crystalline solid. Yield 0.37 g, 67%. ^{1}H NMR (C_6D_6): δ 3.58 (s, 2 H, carborane C–H), 3.35 (s, 12 H, 2 × NMe_2), 2.85 (s, 3 H, NMe), 2.54 (s, 3 H, NMe) and 0.7–1.38 (m, 11 H, C_6H_{11}). Additional peaks in ^{1}H-{^{11}B} NMR (C_6D_6): δ 1.90 (2 H), 2.20 (1 H), 2.50 (1 H), 2.76 (1 H), 2.84 (2 H) and 3.93 (2 H). ^{13}C-{^{1}H} NMR (C_6D_6): δ 211.4 (N–C=N), 58.5 (CH in C_6H_{11}), 50.9 (NMe_2), 50.1 ($C_2B_9H_{11}$), 45.8 (NMe), 40 (NMe), 34.9 (CH_2 in C_6H_{11}) and 25.5 (CH_2 in C_6H_{11}). ^{11}B NMR (C_6D_6): δ 3.2 (d, 1B, J_{B-H} 116), −3.4 (d, 3B, J_{B-H} 124), −8.1 (d, 2B, J_{B-H} 87 Hz), −13.9 (d, 1 B) and −15.6 (d, 2B). Calc. for $C_{15}H_{40}B_9N_4Ta$: C, 32.48; H, 7.27; N, 10.10. Found: C, 32.51; H, 7.47; N, 8.30%. MS: m/z 555 [M^+], 510 [$M - NMe_2^+$] and 402 [$M - (Me_2NC{=}NC_6H_{11})^+$].

[*closo*-3,1,2-Ta(OC$_6$H$_3$Me$_2$-2,6)$_3$(C$_2$B$_9$H$_{11}$)] 7. A stirred toluene (10 cm^3) solution of compound **2** (0.89 g, 2 mmol) was treated dropwise with a toluene solution (10 cm^3) of $HOC_6H_3Me_2$-2,6 (0.9 g, 7.4 mmol). The yellow solution was refluxed for 12 h. The reaction mixture then allowed to cool to room temperature and the solvent evaporated under reduced pressure. The pale yellow residue was extracted with fresh toluene (10 cm^3), filtered and carefully layered with pentane (10 cm^3). Slow recrystallisation at −20 °C produced colourless crystals. Yield 1.1 g, 82%. ^{1}H NMR (CD_2Cl_2): δ 2.38 (s, 18 H, $OC_6H_3\mathit{Me}_2$), 3.37 (br s, 2 H, $C_2B_9H_{11}$), 6.97 (t, 6 H, *meta*-H of $C_6H_3Me_2$) and 7.11 (d, 3 H, *para*-H of $C_6H_3Me_2$). Additional peaks in ^{1}H-{^{11}B} NMR (300 MHz, CD_2Cl_2): δ 1.21 (1 H), 2.31 (2 H), 2.36 (2 H), 2.66 (2 H), 2.89 (1 H) and 3.07 (1 H). ^{13}C-{^{1}H} NMR (CD_2Cl_2): δ 17.4 (*Me*Ar), 60.3 (br, $C_2B_9H_{11}$), 124.7 (*para*-C of $OC_6H_3Me_2$), 128.7 (*ortho*-C of $OC_6H_3Me_2$), 129.4 (*meta*-C of $OC_6H_3Me_2$) and 158.6 (*ipso*-C of $OC_6H_3Me_2$). ^{11}B NMR (96.2 MHz, CD_2Cl_2): δ 7.3 (d, 1B, J_{B-H} 138), 0.7 (d, 2B, J_{B-H} 138), −3.4 (d, 2B, J_{B-H} 138), −9.2 (d, 3 B) and −15.3 (d, 1B, J_{B-H} 172 Hz). Calc. for $C_{26}H_{38}B_9O_3Ta$: C, 46.14; H, 5.66. Found: C, 45.9; H, 5.63%.

[*closo*-3-Ta(SC$_6$H$_5$)$_4$(9-NHMe$_2$-1,2-C$_2$B$_9$H$_{10}$)] 8. A stirred toluene (10 cm^3) solution of compound **2** (0.89 g, 2 mmol) was cooled to −60 °C and treated dropwise with a toluene solution (10 cm^3) of PhSH (0.88 g, 8 mmol). On warming the yellow solution to ambient temperature it rapidly turned blood red. The reaction mixture was then stirred at room temperature for 12 h, after which the solvent was evaporated under reduced pressure. The red residue was extracted with toluene (10 cm^3), filtered and carefully layered with pentane (10 cm^3). Slow recrystallisation at −20 °C produced deep red crystals. Yield 0.84 g, 53%. ^{1}H NMR (CD_2Cl_2): δ 3.19 (s, 2 H, $H_2C_2B_9H_8$-$NHMe_2$), 3.27 (s, 6 H, NMe_2), 3.49 (br s, NH) and 7.11–7.30 (M, 4 × SPh). Additional peaks in ^{1}H-{^{11}B} NMR (CD_2Cl_2): δ 3.11 (1 H), 2.86 (2 H), 2.394 (2 H), 1.99 (1 H) and 1.58 (2 H). ^{13}C-{^{1}H} NMR (CD_2Cl_2): δ 50.3 (NMe_2), 56.3 (br, $C_2B_9H_{10}$-$NHMe_2$), 127.7 (*para*-C of SPh), 128.8 (*meta*-C of SPh), 132.5 (*ortho*-C of SPh) and 143.1 (*para*-C of SPh). ^{11}B NMR (CD_2Cl_2): δ 23.3 (s, 1B), −3.4 (d, 2B, J_{B-H} 124), −4.4 (d, 2B, J_{B-H} 113), −8.7 (d, 2B, J_{B-H} 172), −10.5 (d, 1B, J_{B-H} 157) and −16.3 (d, 1B, J_{B-H} 117). Calc. for $C_{28}H_{37}B_9NS_4Ta{\cdot}0.2C_7H_8$: C, 43.4; H, 4.8; N, 1.7. Found: C, 43.5; H, 5.0; N, 1.6%.

X-Ray crystallography

Single-crystal diffraction experiments at 150 K (**3**, **5** and **7**) or 120 K (**4** and **8**) were carried out with a SMART 1K CCD area detector, using graphite-monochromated Mo-Kα radiation ($\bar{\lambda}$ = 0.71073 Å). The reflection intensities were corrected for absorption by numerical integration based on measurements of the crystal and face indexing (for compounds **7** and **8**, using SHELXTL software[42]) or by a semi-empirical method based on multiple scans of identical reflections and Laue equivalents using the SADABS program for **4** and **5**,[43] and using SHELXTL for **3**. The structures were solved by direct methods and refined by full-matrix least squares against F^2 of all data, using SHELXTL programs.[42] Crystal data and experimental details are listed in Table 4.

CCDC reference number 186/2165.

See http://www.rsc.org/suppdata/dt/b0/b004862n/ for crystallographic files in .cif format.

Acknowledgements

We acknowledge the award of an EPSRC Senior Research Fellowship to J. A. K. H. and we thank EPSRC and Kvaerner Process Technology for a CASE studentship to A. L. J. We thank the ERDF-funded 21st Century Materials Centre at the University of Durham for a fellowship to J. M. M.

References

1 A. S. Batsanov, A. V. Churakov, J. A. K. Howard, A. K. Hughes, A. L. Johnson, A. J. Kingsley, I. S. Neretin and K. Wade, *J. Chem. Soc.*, *Dalton Trans.*, 1999, 3867.

2 R. Uhrhammer, D. J. Crowther, J. D. Olson, D. C. Swenson and R. F. Jordan, *Organometallics*, 1992, **11**, 3098.

3 D. J. Crowther, R. A. Fisher, A. M. Canich, G. G. Hlatky and H. W. Turner, *US Pat.*, 5502124, 1996; D. J. Crowther, S. L. Borkowsky, D. Swenson, T. Y. Meyer and R. F. Jordan, *Organometallics*, 1993, **12**, 2897; D. J. Crowther, D. C. Swenson and R. F. Jordan, *J. Am. Chem. Soc.*, 1995, **117**, 10403.

4 D. E. Bowen, R. F. Jordan and R. D. Rogers, *Organometallics*, 1995, **14**, 3630.
5 G. Chandra and M. F. Lappert, *J. Chem. Soc. A*, 1968, 1940; M. F. Lappert, P. P. Power, A. R. Sanger and R. C. Srivastava, *Metal and Metalloid Amides*, Ellis Horwood Publishers, Chichester, 1980; M. H. Chisholm and I. P. Rothwell, in *Comprehensive Co-ordination Chemistry*, eds. G. Wilkinson R. D. Gillard and J. A. McCleverty, Pergamon Press, Oxford, 1987, vol. 2, ch. 13.4.
6 A. K. Hughes, A. Meetsma and J. H. Teuben, *Organometallics*, 1993, **12**, 1936.
7 W. A. Hermann and W. Baratta, *J. Organomet. Chem.*, 1996, **506**, 357; Y. Mu, W. E. Piers, M. A. MacDonald and M. J. Zaworotko, *Can. J. Chem.*, 1995, **73**, 2233; Y. Mu, W. E. Piers, D. C. MacQuarrie, M. J. Zaworotko and V. G. Young, *Organometallics*, 1996, **15**, 2720; Z. Ziniuk, I. Goldberg and M. Kol, *J. Organomet. Chem.*, 1997, **546**, 441.
8 I. A. Guzei, A. G. Baboul, G. P. A. Yap, A. L. Rheingold, H. B. Schlegel and C. H. Winter, *J. Am. Chem. Soc.*, 1997, **119**, 3387; I. A. Guzei, G. P. A. Yap and C. H. Winter, *Inorg. Chem.*, 1997, **36**, 1738; Y. Mu, W. E. Piers, L. R. Macgillivray and M. J. Zaworotko, *Polyhedron*, 1995, **14**, 1.
9 G. M. Diamond, R. F. Jordan and J. L. Petersen, *Organometallics*, 1996, **15**, 4045; J. N. Christopher, G. M. Diamond, R. F. Jordan and J. L. Petersen, *Organometallics*, 1996, **15**, 4038; G. M. Diamond, R. F. Jordan and J. L. Petersen, *J. Am. Chem. Soc.*, 1996, **118**, 8024.
10 For an example of the balance between kinetic and thermodynamic control see: A. K. Hughes and A. J. Kingsley, *J. Chem. Soc.*, *Dalton Trans.*, 1997, 4139.
11 K. Jones and M. F. Lappert, *J. Organomet. Chem.*, 1965, **3**, 295.
12 C. Chandra, A. D. Jenkins, M. F. Lappert and R. C. Srivastava, *J. Chem. Soc. A*, 1970, 2550.
13 J. Barker and M. Kilner, *Coord. Chem. Rev.*, 1994, **133**, 219.
14 For examples containing lithium see: D. R. Armstrong, D. Barr, R. Snaith, W. Clegg, R. E. Mulvey, K. Wade and D. Reed, *J. Chem. Soc.*, *Dalton Trans.*, 1987, 1071; R. P. Davies, P. R. Raithby, G. P. Shields, R. Snaith and A. E. H. Wheatley, *Organometallics*, 1997, **16**, 2223.
15 U. Segerer, S. Blaurock, J. Sieler and E. Hey-Hawkins, *Organometallics*, 1999, **18**, 2838; Z. Hou and D. W. Stephan, *J. Am. Chem. Soc.*, 1992, **114**, 10088.
16 L. D. Durfee and I. P. Rothwell, *Chem. Rev.*, 1988, **88**, 1059.
17 For an example involving a carborane spectator ligand see: E. A. Boring, M. Sabat, M. G. Finn and R. N. Grimes, *Organometallics*, 1997, **16**, 3993.
18 A. Dormond, A. Aaliti and C. Moïse, *J. Chem. Soc.*, *Chem. Commun.*, 1985, 1231; P. Zanella, N. Brianese, U. Casellato, F. Ossola, M. Porchia, G. Rossetto and R. Graziani, *J. Chem. Soc.*, *Dalton Trans.*, 1987, 2039; M. H. Chisholm, C. E. Hammond, D. Ho and J. C. Huffman, *J. Am. Chem. Soc.*, 1986, **108**, 7860; Z. Z. Wu, J. B. Diminne and Z. L. Xue, *Organometallics*, 1999, **18**, 1002; M. Galakhov, P. Gómez-Sal, A. Martín, M. Mena and C. Yélamos, *Eur. J. Inorg. Chem.*, 1998, 1319; Z. Wu, J. B. Diminnie and Z. Xue, *Organometallics*, 1999, **18**, 1002.
19 V. C. Gibson, *J. Chem. Soc.*, *Dalton Trans.*, 1994, 1607.
20 R. N. Grimes, in *Comprehensive Organometallic Chemistry II*, ed. E. W. Abel, F. G. A. Stone and G. Wilkinson, Pergamon Press, Oxford, 1995, vol. 1, ch. 9; M. F. Hawthorne, *Acc. Chem. Res.*, 1968, **1**, 281; A. K. Saxena and N. S. Hosmane, *Chem. Rev.*, 1993, **93**, 1081.
21 Z. G. Lewis, D. Reed and A. J. Welch, *J. Chem. Soc.*, *Dalton Trans.*, 1992, 731; U. Grädler, A. S. Weller, A. J. Welch and D. Reed, *J. Chem. Soc.*, *Dalton Trans.*, 1996, 335.
22 D. E. Smith and A. J. Welch, *Organometallics*, 1986, **5**, 760.
23 F. Teixidor, S. Gómez, M. Lamrani, C. Viñas, R. Sillanpää and R. Kivekäs, *Organometallics*, 1997, **16**, 1278; S. Gómez, C. Viñas, M. Lamrani, F. Teixidor, R. Kivekäs and R. Sillanpää, *Inorg. Chem.*, 1997, **36**, 3565; M. Lamrani, S. Gómez, C. Viñas, F. Teixidor, R. Sillanpää and R. Kivekäs, *New J. Chem.*, 1996, **20**, 909.
24 J. Cowie, E. J. M. Hamilton, J. C. V. Laurie and A. J. Welch, *J. Organomet. Chem.*, 1990, **394**, 1.
25 C. Boisson, J. C. Berthet, M. Ephritikine, M. Lance and M. Nierlich, *J. Organomet. Chem.*, 1996, **522**, 249.
26 C. Boisson, J. C. Berthet, M. Lance, M. Nierlich and M. Ephritikine, *J. Organomet. Chem.*, 1997, **548**, 9.
27 D. J. Cardin and M. F. Lappert, *Chem. Commun.*, 1967, 1034.
28 L. Wesemann, M. Trinkaus and M. Ruck, *Angew. Chem.*, *Int. Ed.*, 1999, **38**, 2375.
29 T. A. George, K. Jones and M. F. Lappert, *J. Chem. Soc. A*, 1969, 992.
30 A. S. F. Boyd, G. M. Rosair, F. B. H. Tiarks, A. S. Weller, S. K. Zahn and A. J. Welch, *Polyhedron*, 1998, **17**, 2627; G. M. Rosair, A. J. Welch, A. S. Weller and S. K. Kahn, *J. Organomet. Chem.*, 1997, **536**, 299; M. Gomez Saso, D. F. Mullica, E. Sappenfield and F. G. A. Stone, *Polyhedron*, 1996, **15**, 793; Y. K. Yan, D. M. P. Mingos, T. E. Muller, D. J. Williams and M. Kurmoo, *J. Chem. Soc.*, *Dalton Trans.*, 1995, 2509; Y. K. Yan, D. M. P. Mingos, T. E. Muller, D. J. Williams and M. Kurmoo, *J. Chem. Soc.*, *Dalton Trans.*, 1994, 1735; D. F. Mullica, E. L. Sappenfield, F. G. A. Stone and S. F. Woolam, *Organometallics*, 1994, **13**, 157; E. J. M. Hamilton and A. J. Welch, *Polyhedron*, 1991, **10**, 471; J. Cowie, E. J. M. Hamilton, J. C. V. Laurie and A. J. Welch, *J. Organomet. Chem.*, 1990, **394**, 1.
31 S. B. Miller and M. F. Hawthorne, *J. Chem. Soc.*, *Chem. Commun.*, 1976, 787; R. E. King III, S. B. Miller, C. B. Knobler and M. F. Hawthorne, *Inorg. Chem.*, 1983, **22**, 3548.
32 G. M. Rosair, A. J. Welch, A. S. Weller and S. K. Zahn, *J. Organomet. Chem.*, 1997, **536**, 299; S. A. Jasper, J. C. Huffman and L. J. Todd, *Inorg. Chem.*, 1998, **37**, 6060; S. A. Batten, J. C. Jeffery, L. H. Rees, M. D. Rudd and F. G. A. Stone, *J. Chem. Soc.*, *Dalton Trans.*, 1998, 2839.
33 C. J. Jones, J. N. Francis and M. F. Hawthorne, *J. Am. Chem. Soc.*, 1973, **95**, 7633; M. R. Churchill and K. Gold, *Inorg. Chem.*, 1973, **12**, 1157; J. Plešek, B. Štíbr and S. Heřmánek, *Collect. Czech. Chem. Commun.*, 1984, **49**, 1492.
34 M. F. Hawthorne, L. F. Warren Jr., K. P. Callahan and N. F. Travers, *J. Am. Chem. Soc.*, 1973, **95**, 7633.
35 H. C. Kang, S. S. Lee, C. B. Knobler and M. F. Hawthorne, *Inorg. Chem.*, 1991, **30**, 2024; R. E. King III, S. B. Miller, C. B. Knobler and M. F. Hawthorne, *Inorg. Chem.*, 1983, **22**, 3548.
36 F. H. Allen and O. Kennard, *Chem. Des. Autom. News*, 1992, **8**, 1; F. H. Allen and O. Kennard, *Chem. Des. Autom. News*, 1992, **8**, 31.
37 H. Nöth and M. Schmidt, *Organometallics*, 1995, **14**, 6601.
38 O. J. Curnow, M. D. Curtis, A. Rheingold and B. S. Haggerty, *Inorg. Chem.*, 1991, **30**, 4043.
39 K. Tatsumi, I. Matsubara, Y. Inoue, A. Nakamura, K. Miki and N. Kasai, *J. Am. Chem. Soc.*, 1989, **111**, 7766.
40 S. M. Koo, R. Bergero, A. Salifoglou and D. Coucouvains, *Inorg. Chem.*, 1990, **29**, 4844.
41 P. Kubáček, R. Hoffmann and Z. Havalas, *Organometallics*, 1982, **1**, 180.
42 SHELXTL, Version 5.1 NT, Brüker AXS, Analytical X-ray Systems, Madison, WI, 1998.
43 G. M. Sheldrick, SADABS, Program for scaling and correction of area detector data, University of Göttingen, 1996.